Soils and Rocks
An International Journal of Geotechnical and Geoenvironmental Engineering
www.soilsandrocks.com
ISSN 1980-9743
ISSN-e 2675-5475

Numerical analysis of the behavior of piled rafts and pile groups in the presence of pile defects

Felipe Carlos de Araújo Leal[1#], Osvaldo de Freitas Neto[2],
Wilson Cartaxo Soares[3], Roberto Quental Coutinho[4], Renato Pinto da Cunha[5]

Article

Keywords
Numerical analysis
Piled raft
Pile foundation
Pile defect
Foundation engineering

Abstract

This article aims to evaluate the behavior of piled rafts and pile groups subject to the presence of defective piles. To simulate the defect, it was considered that a foundation pile is shorter than projected. Seven static load tests performed in 2011 in the city of João Pessoa, in north-east Brazil, were used as the basis of analysis. These load tests were performed on an isolated raft, in 3 piled rafts and in 3 pile groups. In this study, the ELPLA® software, based on a hyperbolic iterative model, was used. Initially, modeling was performed for the original situations with intact foundations, and the results were compared with previous experimental results. Afterwards, numerical modeling was performed considering four defect levels, which correspond to a decrease in the pile length. According to the results obtained, it could be observed that, due to the presence of the defect, there was a reduction in the stiffness and load capacities of all the foundations analyzed, the occurrence of differential settlements in the foundations, and an increase in the load absorbed by the raft in the piled rafts.

1. Introduction

Increasingly intense occupation of urban space can be observed as a historical trend in Brazilian cities. This dynamic reduces the space available to construct to such an extent that buildings are built on smaller plots of land, becoming taller and leaner. As a result, the demands imposed by the superstructure on the foundation system become increasingly high and complex, which makes it necessary to compatibilizer designs and make use of more efficient, better performing foundation systems to support these demands, ensuring greater safety and cost reduction.

In current foundation engineering practices, some simplifications are allowed when designing a pile foundation system. One hypothesis used to facilitate the study and modeling of the problem is that the bearing superficial block (or raft) only has the function of transmitting superstructure loads to the piles, serving as a transition element between them. In this case, the contribution of the block to the load capacity of the foundation is not considered.

Given the simplification mentioned above, commonly adopted in design, in a foundation system constituted by a pile group, the load capacity is provided by the stresses distributed by the pile shaft (lateral frictional resistance) and the stresses distributed by the pile tip (tip resistance). In a piled raft, the contribution of the superficial element to the load capacity of the system is considered. Thus, the load capacity is given by the lateral friction and the pile tip resistance, as well as by the stresses distributed by the raft base (superficial element).

Although it is expected that piled rafts may lead to a cost reduction and efficiency in the foundation's performance, there is still a noticeable restriction when using them. One explanation for this is that piled raft modelling is more complex, involves more interactions than conventional pile group modelling and there is relatively little experience, particularly in Brazil. Another explanation may lie in the fact that the Brazilian foundation standard, NBR 6122 (ABNT, 2019), although allowing the use of piled rafts, does not explicitly include this modality in its text, and designers generally want to ensure a conservative resistance in the foundation (designing traditionally), hence safeguarding against structural element defects or unpredictable variability in soil characteristics. Studying the foundation behavior

#Corresponding author. E-mail address: felipe.leal@ifce.edu.br
[1]Instituto Federal do Ceará, Crateús, CE, Brasil.
[2]Universidade Federal do Rio Grande do Norte, Departamento de Engenharia Civil, Natal, RN, Brasil.
[3]Concresolo & Copesolo Geotecnia e Fundações, João Pessoa, PB, Brasil.
[4]Universidade Federal de Pernambuco, Departamento de Engenharia Civil, Recife, PE, Brasil.
[5]Universidade de Brasília, Departamento de Engenharia Civil e Ambiental, Brasília, DF, Brasil.

Submitted on November 18, 2024; Final Acceptance on May 6, 2025; Discussion open until August 31, 2025.
Editor: Renato P. Cunha
https://doi.org/10.28927/SR.2025.001124

when there are defects is important because it can evaluate the important role that the superficial element (raft) plays in the system´s performance in these situations.

This paper aims to numerically evaluate the behavior of piled rafts and pile groups, based on sandy soils typical of northeastern Brazil, in the presence of pile defects, using the ELPLA® software, version 10.1. The defect analyzed in this article was the presence of a pile shorter than the designed length, which is a common occurrence in foundation pathologies. For instance, Klingmüller & Kirsch (2004) found that 21% of the pathologies, in 25 years of integrity tests in Germany, were caused by insufficient foundation length. Numerical modeling was performed considering variations in the length of a pile in order to verify its influence on the stiffness, load capacity and load mobilization mechanisms of the foundations.

2. Piled rafts: case studies of pile defects

A piled raft is a type of mixed foundation, that is, it results from joining a shallow foundation (block/raft) with a deep foundation (piles). The performance of a piled raft foundation is the result of the efforts mobilized by the pile tip and shaft, as well as the raft base.

The good performance of a foundation depends on the geotechnical conditions of the subsoil and the integrity of the structural elements. According to Poulos (2001), the favorable situation for using piled rafts corresponds to soil profiles consisting of stiff clay and/or compact sand, especially in the most superficial layers of soil. However, even under favorable conditions, the piled foundations may be subject to defects that affect their behavior. Depending on the type and magnitude of the defect, its presence can lead to the collapse of a foundation system.

Defects in piled foundations can be of geotechnical or structural origin. According to Poulos (1999), defects of geotechnical origin are related to the presence of compressible material layers and low resistance adjacent to the pile, residues in the pile tip, and presence of bentonite mud in the pile shaft, among others. Structural problems are related to lower strength concrete in pile regions, necking in the pile shaft, damaged areas, smaller dimensions in structural elements, among others. In this article, distinct performance scenarios were simulated where there is a shorter than expected pile, which is configured as a situation of structural defect and/or construction pathology, as described in chapter 3.2.

Various studies can be cited in scientific literature that address piled foundations subject to the presence of defective piles. The following studies can be mentioned as examples: Poulos (1997), Abdrabbo (1997), Poulos (1999), Xu (2000), Kong & Zhang (2004), Poulos (2005), Cordeiro (2007), Cunha et al. (2007), Zhang & Wong (2007), Cunha et al. (2010), Leung et al. (2010), Freitas Neto (2013), Albuquerque et al. (2017), Alva (2017), Cordeiro (2017), Xu et al. (2019), Freitas Neto et al. (2020), Yan et al. (2020) and García et al. (2023).

Regarding the most recent studies, Freitas Neto et al. (2020) carried out numerical (finite element method) and experimental studies, on a full-scale case, in a raft with a defective pile founded on a tropical soil in Brazil. The defect considered was the necking of the shaft, with the subsequent decrease in structural strength and stiffness of the shaft. The authors noted that the defect in the pile resulted in a decrease in the load capacity and the safety factor of the foundation. Yan et al. (2020) also carried out experimental, centrifuge, and numerical studies, using the finite element method, to investigate the lateral load capacity performance of a pier supported by defective piles. García et al. (2023) investigated, through experimental and numerical methods, the effects of defective piles in horizontally loaded piled raft foundations. The results show that the presence of a defective pile increases the raft tilting.

3. Materials and methods

3.1 Experimental program

Soares et al. (2015), from the D.Sc. thesis of Soares (2011), conducted four Standard Penetration Tests (SPT) and seven slow static load tests on isolated raft, piled raft and pile group foundations in the city of João Pessoa, north-east Brazil (Figure 1). An isolated raft, and piled rafts with one, two and four piles were tested, as well as a pile group also consisting of one, two and four piles. Thus, overall, the author executed 14 hollow auger piles whose length and diameter were 4.5 meters and 0.30 meters, respectively. The dimensions of the block/raft positioned at the top of the piles were 1.55 m x 1.55 m x 0.85 m. Details about the execution of the hollow auger piles can be seen in Soares et al. (2015). Figure 2 shows the position of the tested foundations, as well as the location of the SPT's holes.

Based on the results of the SPT's, Soares et al. (2015) established the representative subsoil profile, with the mean values of the penetration resistance index (N_{SPT}) along the depth (Figure 3). It is observed that the subsoil is typically sandy.

3.2 Numerical modelling

In the present article, the ELPLA® software version 10.1 was used, which presents the possibility of working specifically with piled rafts. A continuous model was considered, in which the soil is represented by a layered medium, with isotropic and elastic behavior and a non-linear hyperbolic model was adopted. The calculation method used in the software was typical for rigid piled rafts. Although the software developer provides details on the calculation method in the manual available on the website, the following is a description of the most relevant aspects of the numerical tool. The main

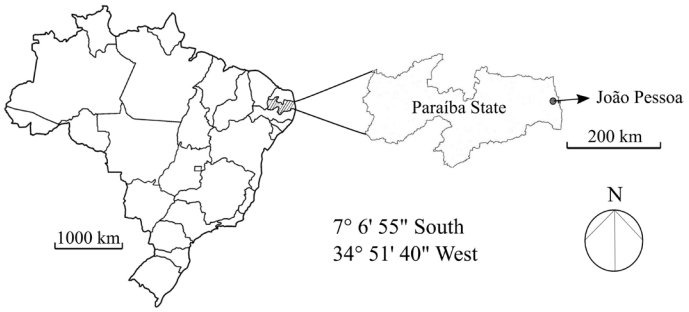

Figure 1. Location of the city of João Pessoa, Brazil.

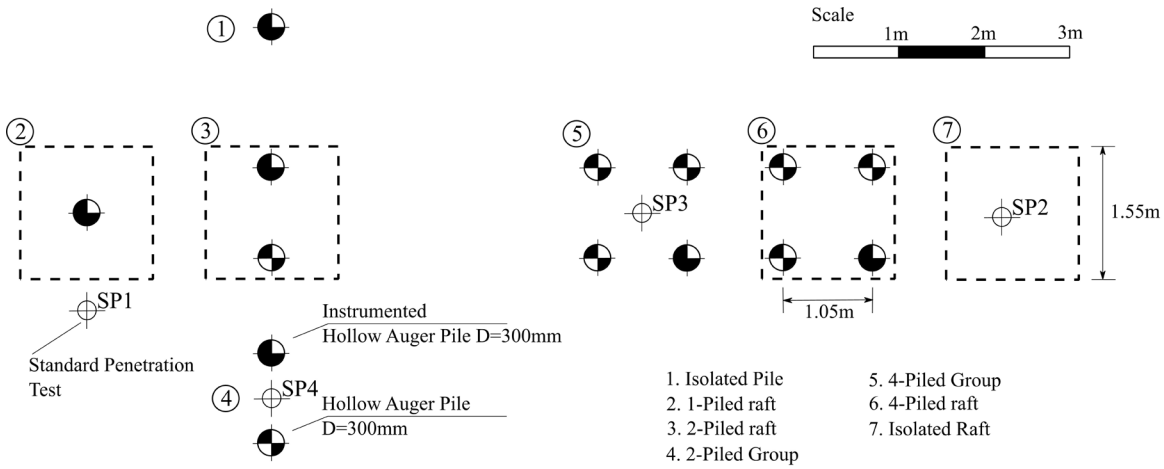

Figure 2. Position of tested foundations and SPT's (Soares et al., 2015).

motivation for using the ELPLA 10.1® software is because of its reduced processing time and the fact that it is easy to use. The ELPLA 10.1® software presents a calculation model in which the raft and the piles are divided into nodes whose number is defined by the user. Thus, the software establishes a system of equations that relates, at each node, the contact force (Q) to the soil stiffness (k) and settlement (w). For the general foundation scheme shown in Figure 4, the relationship between settlements and contact forces of the piled raft can be written in the form of a general compacted matrix as follows (Equation 1):

$$\{Q\} = [k] \cdot \{w\} \tag{1}$$

where: $\{w\}$ is the settlement vector; $\{Q\}$ is the contact force vector; and $[k]$ is the soil stiffness matrix of the piled raft.

In the analysis of rigid piled rafts, the Equation 2 expresses the settlement (w_i) in each raft node or in a pile, which have coordinates (x_i, y_i) in relation to the centroid of the raft geometry, as a function of the rigid body translation of the piled raft (w_c) and the rigid body rotations (θ_x and θ_y) of the piled raft about the axes of the raft geometry centroid.

$$\{w\} = [X]^{\mathrm{T}} \cdot \{\Delta\} \tag{2}$$

where: Δ is the vector of translation w_c and rotations $\tan\theta_x$ and $\tan\theta_y$, and $[X]^{\mathrm{T}}$ is the matrix of $\{1, x_i, y_i\}$, where x_i and y_i are coordinates of node i.

For equilibrium, the sum of the forces applied to each node, as well as the sum of the moments due to these forces, must meet the equilibrium equation (Equation 3):

$$\{N\} = [X] \cdot \{Q\} \tag{3}$$

where: $\{N\}$ is the vector of the resultant forces and moments acting on the piled raft.

Substituting Equations 1 and 2 in Equation 3, the Equation 4 is obtained. Solving this equation, the values of w_c, $\tan\theta_x$, and $\tan\theta_y$ are determined. Thus, from Equation 2, the settlements are found.

$$\{N\} = [X] \cdot [k] \cdot [X]^{T} \cdot \{\Delta\} \tag{4}$$

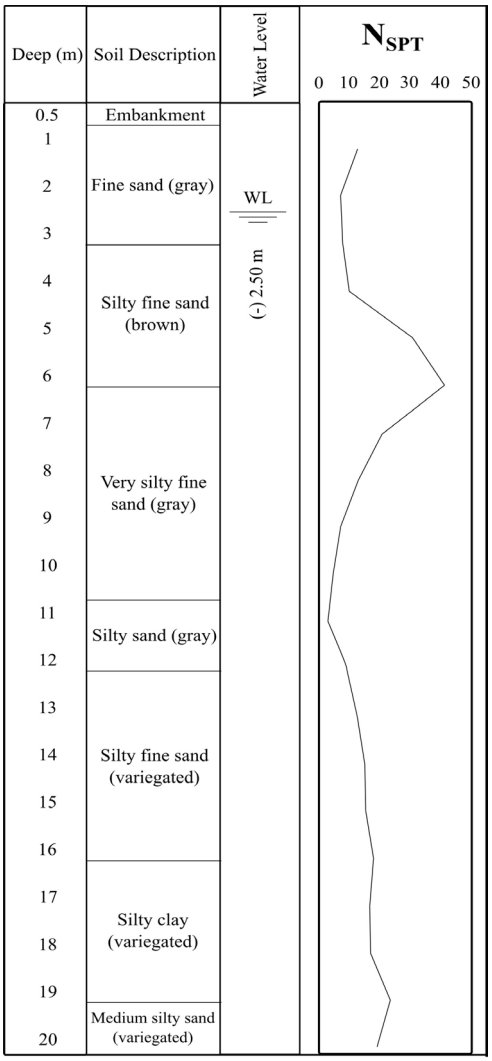

Figure 3. Subsoil profile with N_{SPT} values along the depth (adapted from Soares et al., 2015).

Substituting Equation 2 in Equation 1, it is possible to determine the pile loads and the contact forces, using the Equation 5:

$$\{Q\} = [k] \cdot [X]^T \cdot \{\Delta\} \tag{5}$$

After the initial linear analysis, it is possible to determine the settlements $\{w\}$ (Equation 4) and the nodal contact forces $\{Q\}$ (Equation 5) in the piled raft. The nonlinear analysis of the piled raft is based on a hyperbolic formulation through an iterative procedure.

From the computed settlements and contact forces, the nodal stiffness (k_e) at all nodes on the raft and on pile heads is determined using Equation 6.

$$k_e = \frac{Q}{w} \tag{6}$$

The pile stiffness is modified by Equation 7:

$$k_e = \frac{1}{\frac{1}{k} + \frac{w}{Q_l}} \tag{7}$$

where: k is the soil stiffness and Q_l is the limit pile load.

The soil stiffness matrix [k] is converted to the stiffness matrix [k_e]. Thus, after the nonlinear analysis of the piled raft, New settlement values $\{w\}$ are determined. With the new settlement values, new contact force values $\{Q\}$ are determined (equation 6). The procedure described is repeated until there is convergence in the generated settlement values.

Regarding the dimensions of the model, in the horizontal domain the software considers only the dimensions of the raft, while in the vertical domain, a dimension of 3 times the length of the pile was adopted. It is noteworthy that the software's mathematical model only considers the soil beneath the raft foundation, as shown in Figure 4, where the soil and the piles are divided into nodes. Thus, the lateral soil region outside the raft is not taken into account in the mathematical procedure, and therefore, it was not necessary to define a horizontal domain wider than the raft for the model. Figure 5 shows the dimensions of the model.

In this article, initially, numerical analysis was performed for foundations in the intact condition, which were tested by Soares et al. (2015) through static load tests, as discussed in chapter 3.1. These initial analyses were carried out to compare the results of the ELPLA® software with the experimental results and evaluate the convergence of the results, to then expand the analysis considering the presence of defective piles in the foundation. Considering such non-standard piles, the influence of the defect and its magnitude on the load/settlement curves of the foundation systems, the differential settlement, as well as the strength redistribution and load capacity were evaluated. In the present work, the defect considered in the analysis of all the piled foundation models was the presence of a pile shorter than initially predicted, which is 4.5 meters.

For each pile foundation model analysed, the presence of one defective pile and four defect levels were considered, namely: $D_{11\%}$ - 11% reduction in the pile length (4 m defective pile); $D_{33\%}$ - 33% reduction in pile length (3m defective pile); $D_{56\%}$ - 56% reduction in pile length (2 m defective pile); and $D_{78\%}$ - 78% reduction in pile length (1m defective pile). Table 1 presents all the cases considered in this study. Overall, 31 cases were considered, 7 in scenarios with intact piles and 24 in scenarios considering piles with different defect magnitudes. Standard pile groups (PG) differ from piled rafts (PR) in this table, by simply considering or not the raft contact with the superficial soil.

Figure 6 shows the position of the defective pile under the connecting structural element (block/ raft) for the 2-pile and 4-pile foundations. In the case of the 1-piled block/raft, the defective pile represents the unique pile in the foundation system.

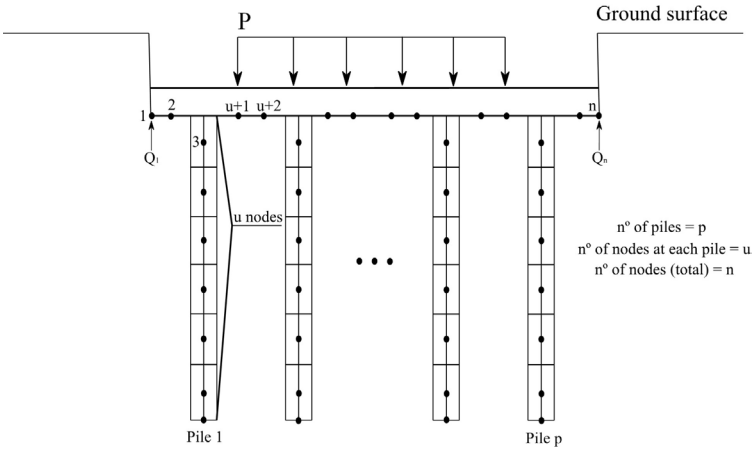

Figure 4. General foundation scheme.

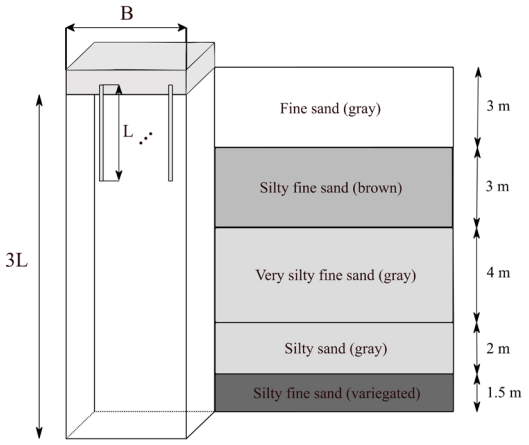

Figure 5. Dimensions of the model.

Table 1. Cases considered in this study.

Intact cases	Defective cases			
R	-	-	-	-
PR_1	$PR_1D_{11\%}$	$PR_1D_{33\%}$	$PR_1D_{56\%}$	$PR_1D_{78\%}$
PR_2	$PR_2D_{11\%}$	$PR_2D_{33\%}$	$PR_2D_{56\%}$	$PR_2D_{78\%}$
PR_4	$PR_4D_{11\%}$	$PR_4D_{33\%}$	$PR_4D_{56\%}$	$PR_4D_{78\%}$
PG_1	$PG_1D_{11\%}$	$PG_1D_{33\%}$	$PG_1D_{56\%}$	$PG_1D_{78\%}$
PG_2	$PG_2D_{11\%}$	$PG_2D_{33\%}$	$PG_2D_{56\%}$	$PG_2D_{78\%}$
PG_4	$PG_4D_{11\%}$	$PG_4D_{33\%}$	$PG_4D_{56\%}$	$PG_4D_{78\%}$

N.B.: R: Raft; PR_i: Piled raft with *i* piles; $PR_iD_{j\%}$: Piled raft with *i* piles and a pile with *j*% shorter length; PG_i: Pile group *i*; $PG_iD_{j\%}$: Pile group *i* and a pile with *j*% shorter length.

Based on the results of the SPT sampling conducted by Soares et al. (2015), shown in Figure 3, the necessary soil parameters for numerical modeling were obtained, according to the following formulations: Modulus of elasticity "E_s" (Teixeira & Godoy, 1996 - 1996 - $E_s = \alpha.K.N$, α and *k* are coefficients that depend on soil type; *N* is the penetration resistance index obtained in the SPT); Friction angle "ϕ" (Teixeira, 1996 - $\phi = \sqrt{20N} + 15$, *N* is the penetration resistance index obtained in the SPT); Specific weight "γ" (Godoy, 1972 apud Cintra et al., 2011); Poisson's ratio "ν" (Godoy, 1972 apud Cintra et al., 2011). Figure 7 shows the simplified geological profile of the subsoil, with the soil

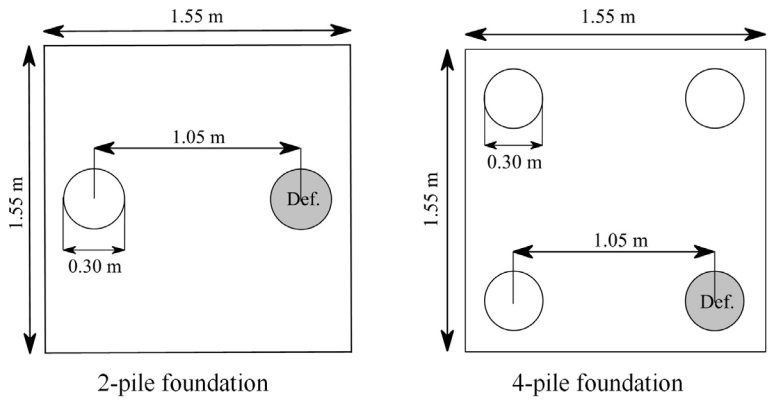

Figure 6. Position of defective pile.

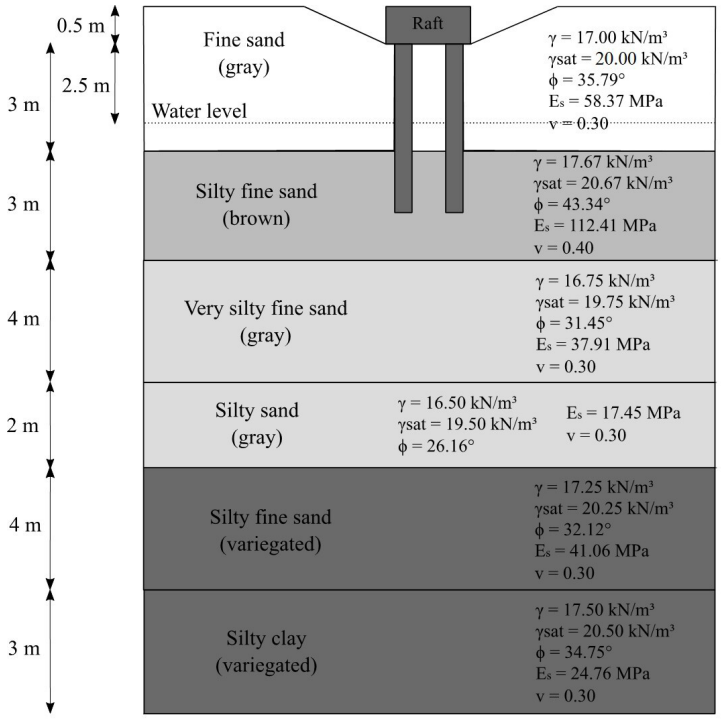

Figure 7. Representative profile and soil parameters.

resistance and deformation parameters per layer. The concrete parameters of the foundation elements were obtained from the Brazilian standard NBR 6118 (ABNT, 2014) using formulations as a function of concrete strength, which was 14.8 MPa (average of the strengths obtained through compression tests on specimens). The remaining parameters were defined as: Modulus of elasticity (E = 21.50 GPa); Specific weight (γ = 25.00 kN/m³); Poisson's ratio (ν = 0.20).

4. Analysis and results

In order to verify the software and input parameters shown in Figure 7, the load tests performed by Soares et al. (2015) were numerically modeled. Figures 8 shows the load versus settlement curves, either in numerical and experimental terms, for the isolated raft and for the foundations with one, two and four piles, respectively. To determine the conventional load capacity (P_{max}), the criteria proposed by Décourt (1993, 1995) and the British Standard (BSI, 2015) were adopted, which indicate that the conventional load capacity for pile foundations is equivalent to the load corresponding to a settlement of 10% of the nominal pile diameter (D), i.e. 30 mm in this case.

Based on the load capacity (P_{max}) a Global Safety Factor (GSF) can be applied to obtain the allowable load (P_a). In this study, a GSF equal to 2 was considered, which is the minimum value recommended by the Brazilian National Standard NBR 6122 (ABNT, 2019) for deep foundations (for conventional pile groups, hence assumed herein equal for piled raft types as well). It is important to note that the

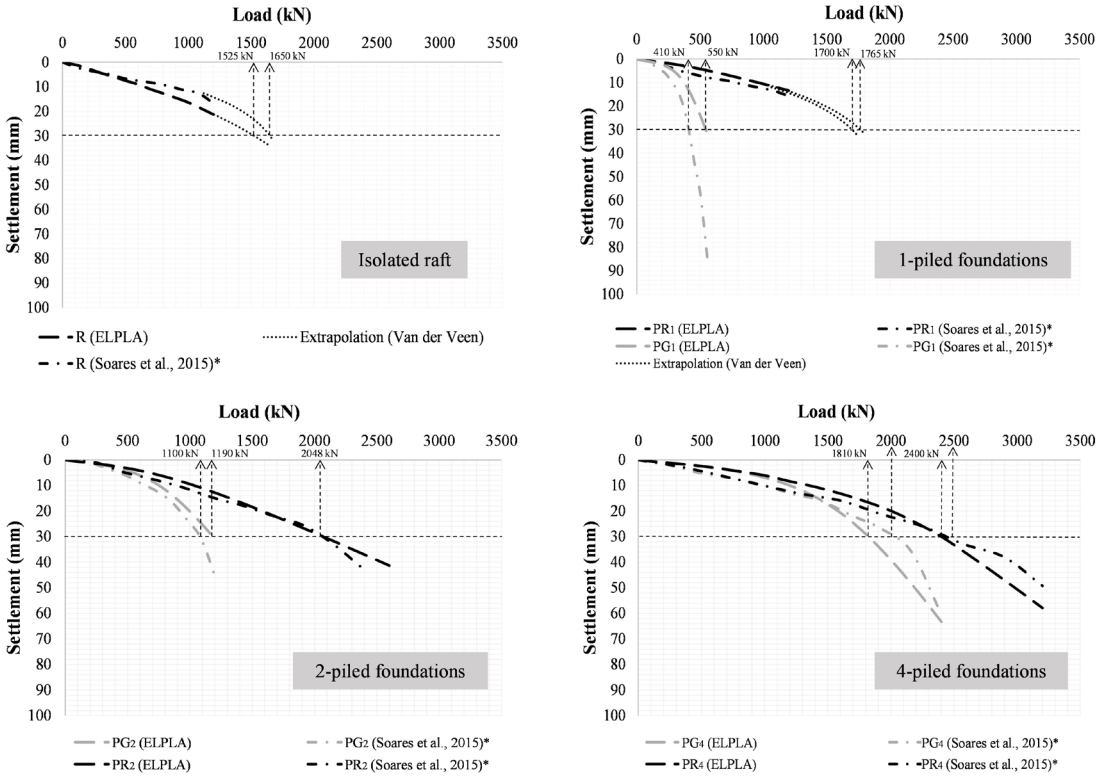

Figure 8. Load/settlement curves (*Experimental Results).

isolated raft and the 1-piled raft did not reach the 30 mm level of settlement, therefore for these types of foundation the load versus settlement curve was extrapolated through the method of van der Veen (1953) to the desired level of settlement.

Table 2 shows the load capacities (P_{max}) and allowable loads (P_a) for all foundation types analyzed using the experimental model proposed by Soares et al. (2015), and the numerical model used in this study. In addition, the load capacities obtained by the two models are compared and it can be seen that the P_{max} variations (δP_{max}) were less than 10% in all the foundations analyzed, except in the PG_1 foundation, where there was a variation of 34.1%. It is also observed that the P_{max} variations were smaller in the piled rafts than in the pile groups, when comparing the numerical and experimental model. The numerical model represents a simplified simulation of what occurs in the field, as verified by the experimental model. In the ELPLA® software, the soil and the piles are represented by nodes, as observed in Chapter 3.2. This may explain the discrepancies found between the numerical and experimental results. However, in general, it can be assumed from Figure 8 that the numerical and experimental load versus settlement curves exhibit similar behavior and converge with each other.

From a global view, considering the results of Figure 8 and Table 2, it can be concluded that the initial geotechnical parameters (Figure 7) led to an adequate closeness between numerical and experimental results, even though some slight divergence was found for the PG_1 case. By evaluating the numerical and experimental load/settlement curves for displacements equivalent to the allowable load (load to which the foundation will be subjected in the field), a greater proximity between the curves was observed, which demonstrates that it is feasible to use the geotechnical parameters of Figure 7 in the modelling process.

After carrying out the comparative analysis of the ELPLA® 10.1 software with Soares et al. (2015) experimental results, modelling was performed considering the presence of a defective pile whose length was shorter than initially predicted. Four defect levels (D11%, D33%, D56%, and D78%) were considered in which the pile length gradually decreases. Figure 9 shows the load versus settlement curves and the load capacities (P_{max}) obtained for the 1-, 2- and 4-piled rafts and pile groups in the above situations. It can be observed that, as predicted, the presence of the defect promotes a reduction in Pmax and in the stiffness of all the foundations analyzed, as they assume higher settlements in relation to the intact situation, for the same load levels applied.

The load capacity of foundations obtained in Figure 9 are depicted in relation to the level of defect in the pile. In addition, Figure 10 shows the percentage reductions in the load capacity of defective foundations when compared to the intact case (ΔP_{max}), for each defect level in the pile. It can be seen that the ΔP_{max} values are higher in the pile groups

Table 2. Load capacities and allowable loads obtained through ELPLA® and the experimental model.

Foundation	ELPLA®		Soares et al. (2015) (experimental)		Comparison of numerical and experimental models
	P_{max} (kN)	P_a (kN)	P_{max} (kN)	P_a (kN)	δP_{max} (%)*
R	1525.0	762.5	1650.0	825.0	7.6%
PR_1	1765.0	882.5	1700.0	850.0	3.8%
PR_2	2048.0	1024.0	2048.0	1024.0	0%
PR_4	2400.0	1200.0	2500.0	1250.0	4.0%
PG_1	550.0	275.0	410.0	205.0	34.1%
PG_2	1190.0	595.0	1100.0	550.0	8.2%
PG_4	1810.0	905.0	2000.0	1000.0	9.5%

N.B.: *$\delta P_{max} = |P_{max,experimental} - P_{max,ELPLA}|/P_{max,experimental}$.

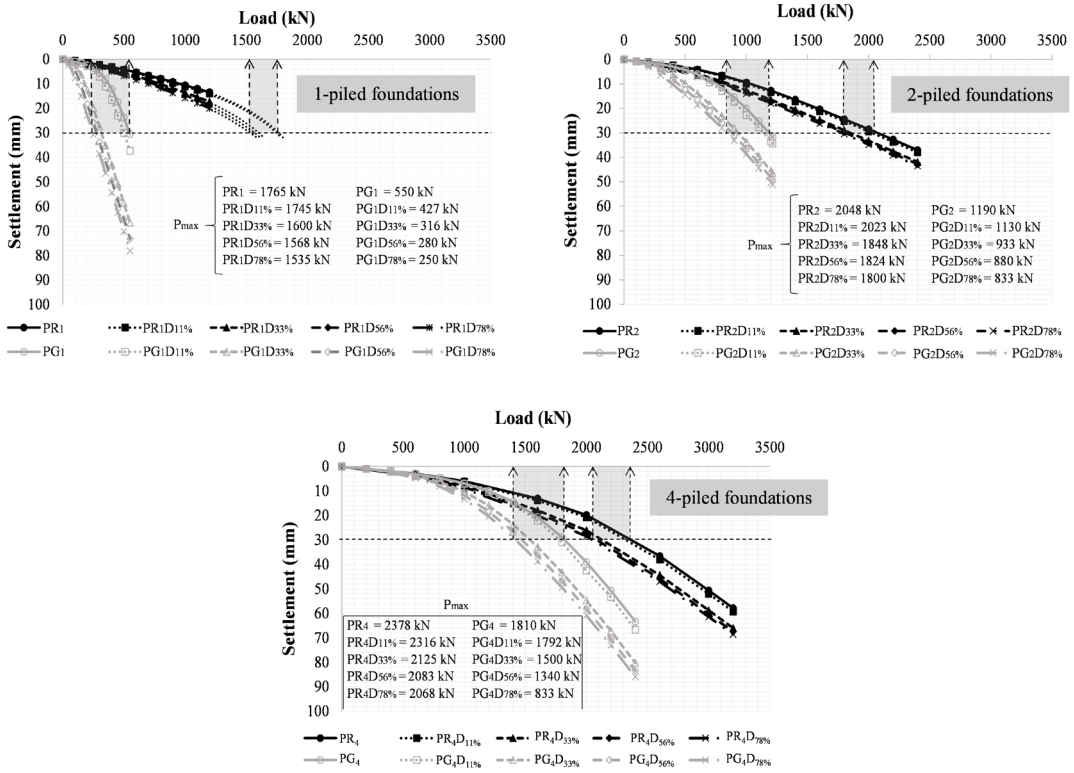

Figure 9. Load/settlement curves and load capacities in defective situation.

than in the piled rafts, which is expected, since in the latter case, the raft is mobilized in order to compensate for the loss of the defective pile resistance, which promotes a lower reduction of Pmax of the foundation. In the case of pile groups, redistribution in mobilized loads does occur, with migration from the defective pile to other piles of the system.

Figure 10 also shows that the greatest loss of load capacity was 55% and occurred in PG1D78%, that is, in the group with 1 pile that was 1 m in length. In the piled raft under the same condition (PR1D78%) the loss of load capacity was 13%, which demonstrates again the positive influence of the raft on the performance of the foundation.

Through Figures 9 and 10, it can be observed that there is a sharper decrease in load capacity and stiffness in all analyzed cases when transitioning from defect D11% to D33%, that is, when the pile length is reduced from 4 m to 3 m. This occurs because, when the pile is shortened to 3 m, it becomes entirely embedded in the fine sand (gray) layer,

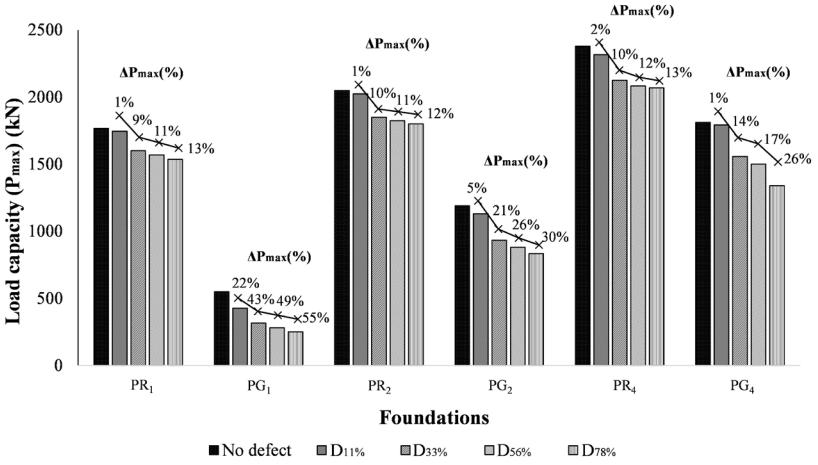

Figure 10. Load capacities of foundations (P_{max}) and their percentage reductions (ΔP_{max}) as a function of the defect level at the pile.

as seen in Figure 6, which has significantly lower resistance and deformability parameters compared to the underlying soil layer, silty fine sand (brown).

Considering the load capacities of all foundations in either intact situation or in the defective four cases, aspects of safety at the rupture of the foundations can be assessed in regard to the defect in the pile. For this, a safety factor was determined for each foundation according to the occurrence of the defect (SF_d), using equation 8:

$$SF_d = \frac{P_{\max}}{S} \tag{8}$$

where: P_{max} is the defective foundation capacity and S is the load applied to the foundation. P_{max} varies according to the defect level in the foundation (as the defect level increases, P_{max} decreases, as seen in Figure 10). It was assumed that the applied load S corresponds to the allowable load of the foundation in the intact condition, numerically assessed, that is, 882.5 kN, 1024 kN and 1200 kN for piled rafts with 1, 2 and 4 piles, respectively and 275 kN, 595 kN and 905 kN for pile groups with 1, 2 and 4 piles, respectively. Thus, in a certain foundation, as the defect level increases, the SF_d decreases, as P_{max} decreases with the increase in the defect. In this case S remains constant, as it is equivalent to the allowable load of the foundation in intact condition.

Figure 11 shows SF_d variations as a function of the defect level in the foundations. It can be observed that when there is no defect, SF_d is equal to 2, which is the expected ideal situation, of intact foundation. When there is a defect, SF_d is less than 2 and decreases as the defect level increases. It can be seen that the group with 1 pile of 1 m in length (PG1D78%) represented the most critical situation, in which SF_d assumed the value of 0.91 and, therefore, indicated a rupture of the foundation.

In Figure 10, it was already noted that this case was the most critical, as it assumed the greatest reduction in load capacity (55%), and this directly interferes with the calculation of the safety factor. The group with a pile of 2 m in length (PG1D56%) is also in a situation of imminent rupture, in which SF_d assumed the value of 1.02. Analyzing the piled rafts under the same conditions (PR1D78% and PR1D56%), it can be observed that the SF_d values are 1.71 and 1.75, respectively, which ensures a satisfactory reserve of resistance even in the presence of the defect. Therefore, the influence of the raft in ensuring the stability of the system is notorious, especially in those cases where there is only one pile in the foundation (SF_d ranged from 0.91 in PG1D78% to 1.71 in PR1D78%, which represents an increase of 88% in the safety factor as a function of the raft-soil contact). Analyzing foundations with 2 and 4 piles at the same defect level, it can be observed that the SF_d varies from 1.4 in the PG2D78% to 1.76 in the PR2D78% (which represents an increase of 26% in SF_d) and from 1.48 in the PG4D78% to 1.74 in the PR4D78% (which indicates an increase of 18% in the safety factor as a function of the raft-soil contact). It can be observed, therefore, that with lesser piles in the foundation, the greater the raft-soil contact contribution, as well as the system's performance.

When loads are applied on a piled raft, one part of the load is mobilized by the raft and the other by the pile(s). Figure 12 shows, for the 1-, 2- and 4-piled rafts, that as the loading level in the foundations increases, the raft will mobilize more load while the piles will have a smaller contribution to the load capacity. This fact was also observed by Lee et al. (2015) in their studies with piled rafts in sand. Alshenawy et al. (2016) also observed that the piles mobilize less load with the increase of loading when the load-settlement behavior is nonlinear. It can also be observed that as the magnitude of the pile defect increases, the raft becomes more mobilized, absorbing more load and tending to compensate for the loss of performance of the defect pile.

As it was done for the determination of SF_d in Figure 11, it was considered that in each foundation a load equivalent

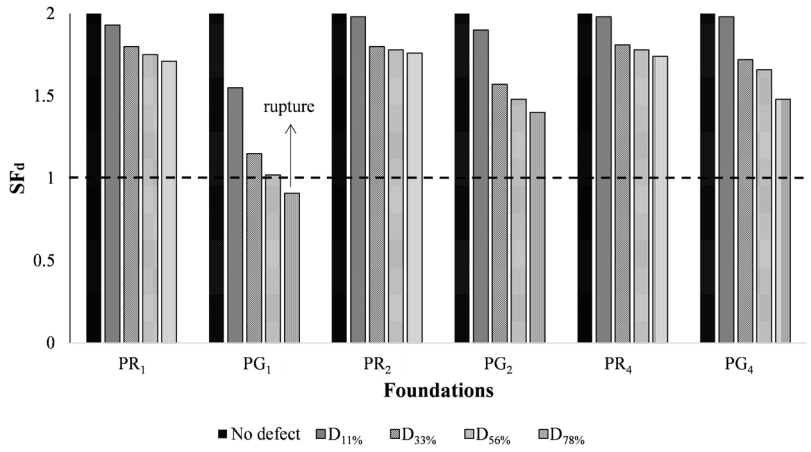

Figure 11. SF_d variation for foundations depending on the level of defect.

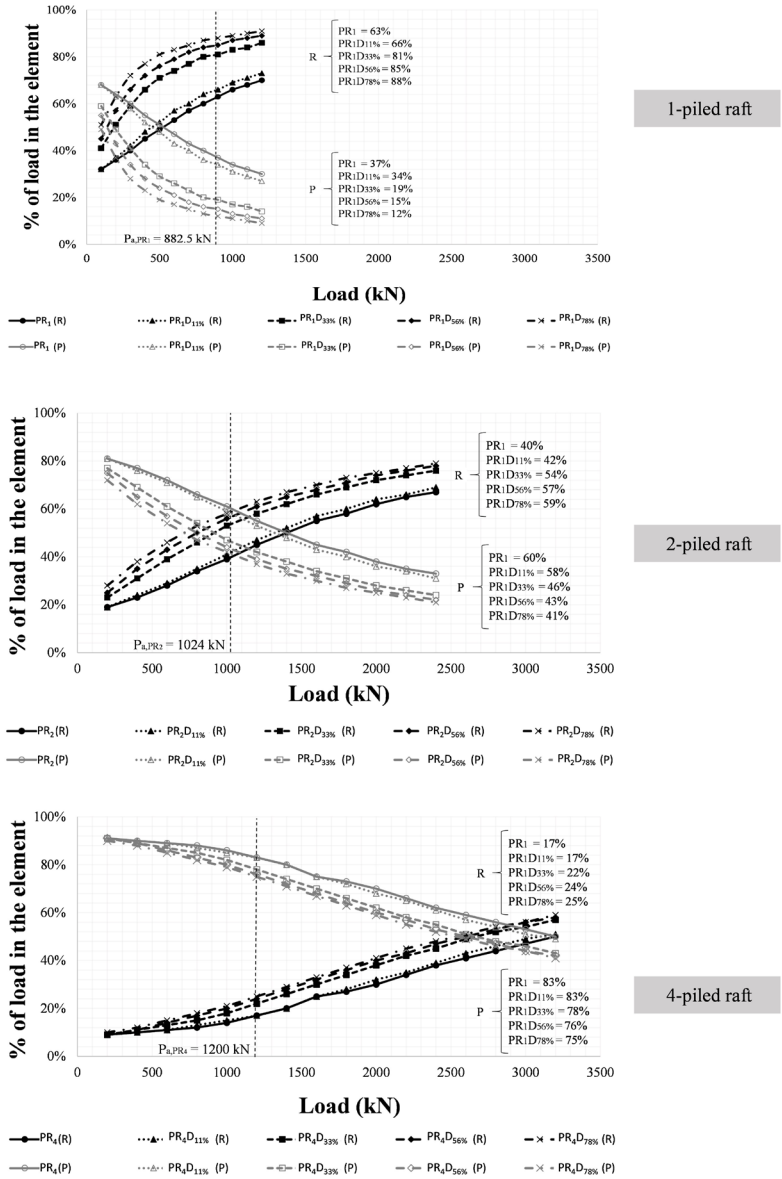

Figure 12. Load mobilization on raft (R) and piles (P) during loading.

to its allowable load in the intact situation (P_a), numerically related, should be applied, that is, 882.5 kN, 1024 kN and 1200 kN for piled rafts with 1, 2 and 4 piles, respectively. Thus, for this level of applied load, Figure 12 highlights the percentage of the load mobilized by the raft (R) and the piles (P) for each defect level, in foundations with 1, 2 and 4 piles, respectively. It can be seen that, in PR1, the raft mobilizes from 63% of the applied load, in the intact situation, to 88%, in the situation with D78% defect, that is, there was an increase of 25% in the load absorbed by the raft in function of the defect. In PR2, this increase was 19% (the raft mobilized 40% of the applied load, in the intact situation, and started to mobilize 59%, in the situation with D78%). Finally, in PR4, there was an increase of 8% in the load absorbed by the raft due to the defect (the raft absorbed 17% of the applied load, in the intact situation, and started to absorb 25%, in the situation with D78%). This fact demonstrates again the importance of the raft on the behavior of the defective foundation and corroborates with aforementioned discussions, regarding the increase of raft contribution with decrease of piles in the system.

The presence of a defective pile in the pile groups and 2- and 4-piled rafts results in differential settlements when loading is applied. The superficial element (block/raft) rotates towards the defective pile which can be measured by calculating the angular distortion (β). Figure 13 shows how the angular distortion in the superficial element varies during loading for the 2- and 4-piled foundations at different defect levels. It is observed that the angular distortions increase with the increase of loading and the defect level in the pile. Also, it is noticed that the angular distortion values are higher in the pile groups than in the piled rafts.

It is considered again that in each foundation a load equivalent to its allowable load in the intact situation (P_a), numerically calculated, is applied, that is 1024 kN for PR2; 595 kN for PG2; 1200 kN for PR4 and 905 kN for PG4. In this case, Figure 13 specifies, for this load level, the angular distortion values as a function of the defect in foundations with 2 and 4 piles, respectively. In this regard, Bjerrum (1963) established boundary distortion values for a foundation as a function of associated damage.

Based on this, it can be observed that the foundations in pile groups PG2D33%, PG2D56%, PG2D78%, PG4D56% and PG4D78% assume angular distortion values of more than 1/100, which results in a situation of high structural damage to buildings and a high potential for rupture. In

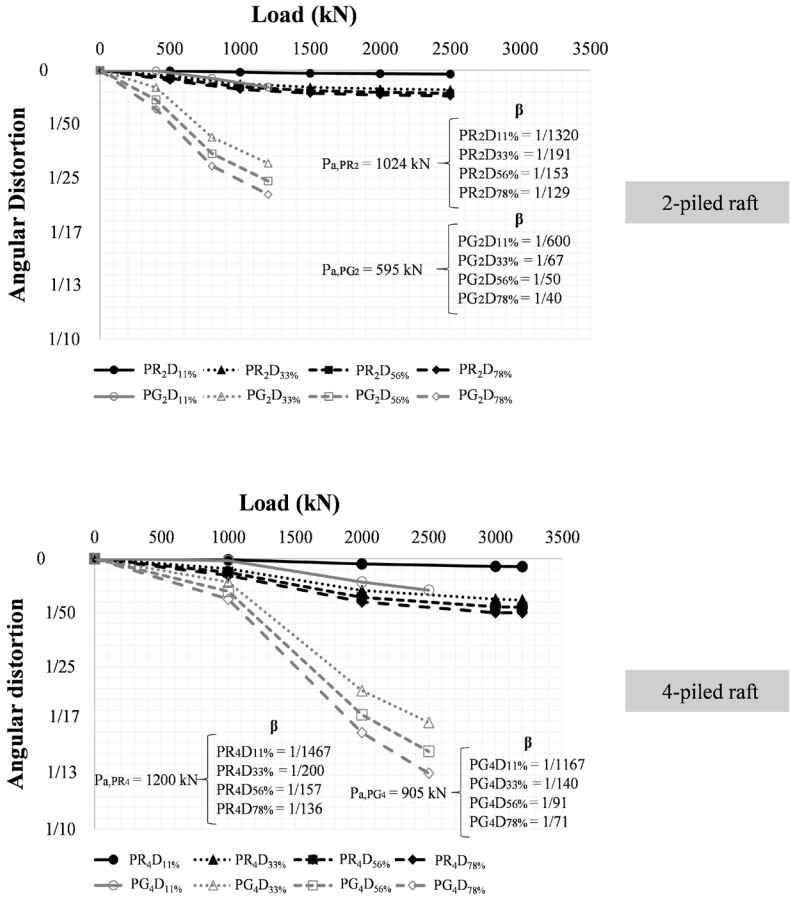

Figure 13. Angular distortion values (β) during loading.

piled raft foundations, the greatest angular distortion found was in PR2D78%, assuming a value of 1/129, which also represents a situation of structural damage in buildings. In the pile groups, the most critical situation was that of PG2D78%, which assumed a value of 1/40. That is, although it still assumes values that would induce the structure to pathological manifestations, the design of the piled raft foundation performed better than the pile group foundation.

5. Conclusions

Considering the analyses performed using the ELPLA® software, version 10.1 regarding the stiffness and load capacity of the intact foundations, it can be observed that the results obtained were in agreement with the experimental results of Soares et al. (2015). Therefore, it is argued that tools with simplified calculation methods, such as the one used in this article, should be encouraged because they attend to the needs of everyday engineering practice, which require speed, agility, and simple models to obtain engineering results.

The main conclusions of this study are presented below:

- When considering the percentage reductions of 11%, 33%, 56% and 78% in the length of the pile, a reduction in the system´s stiffness was observed, and higher settlements appeared for the same applied load levels, as well as a reduction in the load bearing capacities of the foundations. The most critical situation for the piled rafts occurred in PR1D78% (1-piled raft with 78% reduction in pile length), which had a 13% reduction in load capacity, while for the pile groups, the case with a 78% shorter pile (PG1D78%) had a 55% lower load capacity than the intact situation.
- Considering the application in the foundations of a load equivalent to the allowable load of the intact situation (P_a) obtained numerically, the safety factors could be calculated as a function of the presence of the defect (SF_d), relating the load capacity of the defective foundation and the applied load. It could be observed that there was a reduction in the SF_d with an increase in the defect level and, in the PG1D78% situation (group with 1 pile 78% shorter), the rupture was seen, as the SF_d assumed the value of 0.91. The importance that the raft-soil contact represents in the safety of the foundation was notorious, because in all cases of defects the presence of the raft led to an increase in SF_d.
- Regarding the mobilization of loads between elements of the piled rafts, an increase was observed in the mobilization of the superficial element (raft) with the increase in the load and with the increase in the defect level. For a load level equivalent to the allowable load of the foundation with no defect, in the PR1D78% (1-piled raft with 78% reduction in pile length) the raft will mobilize more than 85% of the applied load, characterizing the foundation system´s performance as typical of a piled raft (with partition of load among raft and piles). The importance of the raft in foundation behavior is well known.
- In the 2- and 4 piled- foundations, in situations where there is a pile defect, there were differential settlements that were evaluated by determining the angular distortions. It could be observed that the angular distortions increased when the load and the defect level increased. For a load equivalent to the allowable load of the foundation without defects, in the piled raft foundations the greatest angular distortion found was in PR2D78% (2-piled raft with a 78% shorter pile), which assumed a value of 1/129, while in the pile groups the most critical situation was that of PG2D78% (2-pile group with a 78% shorter pile) with a value of 1/40. Although the raft-soil contact has promoted a reduction in the angular distortion of the foundation, from 1/40 to 1/129, it still represents, in this case, structural damage in buildings.

Based on the analyses performed and the results obtained, it could be concluded in general terms, from the present exercise, that the existence of structural defects in a pile changes the behavior of the group foundation, reducing its stiffness and load capacity. It was clear that piled raft types behave in a better way than conventional pile groups, when a defect is present in one of the piles.

Acknowledgements

The authors are grateful for the support provided by Brazilian organizations that promote research CNPq (National Council for Scientific and Technological Development) and CAPES (Coordination for the Improvement of Higher Education Personnel). This research was also carried out (among other groups) with support from the foundation and in situ testing research group of the Univ. of Brasília, GPFees (https://rpcunha.wixsite.com/gpfees).

Declaration of interest

The authors have no conflicts of interest to declare. All co-authors have observed and affirmed the contents of the paper and there is no financial interest to report.

Authors' contributions

Felipe Carlos de Araújo Leal: conceptualization, methodology, visualization, writing – original draft, writing - review & editing, funding acquisition, resources, supervision. Osvaldo de Freitas Neto: conceptualization, methodology, visualization, writing – original draft, writing - review & editing, funding acquisition, resources, supervision. Wilson Cartaxo Soares: conceptualization, methodology, visualization,

writing - original draft, writing - review & editing, funding acquisition, resources, supervision. Roberto Quental Coutinho: conceptualization, methodology, visualization, funding acquisition, resources, supervision. Renato Pinto da Cunha: visualization, writing – original draft, writing - review & editing, supervision.

Data availability

All data produced or examined in the course of the current study are included in this article.

Declaration of use of generative artificial intelligence

This work was prepared without the assistance of any generative artificial intelligence (GenAI) tools or services. All aspects of the manuscript were developed solely by the authors, who take full responsibility for the content of this publication.

List of symbols and abbreviations

k	Soil stiffness
w	Settlement
D	Pile diameter
E_s	Modulus of elasticity
GSF	Global Safety Factor
N_{SPT}	Penetration resistance index
P_a	Allowable load
P_{max}	Load capacity
Q	Contact force
S	Load applied to the foundation
SF_d	Safety factor with the occurrence of the defect
SPT	Standard Penetration Test
β	Angular distortion
γ	Specific weight
δP_{max} P_{max}	variations
v	Poisson's ratio
ϕ	Friction angle
ΔP_{max}	Percentage reductions in the load capacity of defective foundations when compared to the intact case.

References

Abdrabbo, F.M. (1997). Misuse of soils and foundation causes disaster. In *International Conference on Foundation Failures* (pp. 121-130). Singapore.

ABNT NBR 6118. (2014). *Design of concrete structures: procedure*. ABNT - Associação Brasileira de Normas Técnicas, Rio de Janeiro, RJ (in Portuguese).

ABNT NBR 6122. (2019). *Design and construction of foundations*. ABNT - Associação Brasileira de Normas Técnicas, Rio de Janeiro, RJ (in Portuguese).

Albuquerque, P.J.R., Garcia, J.R., Freitas Neto, O., Cunha, R.P., & Santos Junior, O.F. (2017). Behavioral evaluation of small-diameter defective and intact bored piles subjected to axial compression. *Soils and Rocks*, 40(2), 109-121. http://doi.org/10.28927/SR.402109.

Alshenawy, A.O., Alrefeai, T.O., & Alsanabani, N.M. (2016). Analysis of piled raft coefficient and load-settlement on sandy soil. *Arabian Journal of Geosciences*, 9(6), 475. http://doi.org/10.1007/s12517-016-2494-7.

Alva, F.G. (2017). *Analysis of the behavior of piled rafts with and without defective pile horizontally load in tropical soil* [Doctoral thesis, University of Brasília]. University of Brasília's repository. Retrieved in November 18, 2024, from https://repositorio.unb.br/handle/10482/25226

Bjerrum, L. (1963). Interaction between structure and soil. In *European Conference on Soil Mechanics and Foundation Engineering* (pp. 135-137). Wiesbaden: ECSMFE.

British Standards Institution – BSI. (2015). *BS 8004: 2015: code of practice for foundations.* London.

Cintra, J.C.A., Aoki, N., & Albiero, J.H. (2011). *Fundações diretas: projeto geotécnico*. São Paulo: Oficina de Textos.

Cordeiro, A.F. (2017). *Modelagem física de radiers estaqueados com e sem estacas defeituosas assentes em areia* [Doctoral thesis, University of Brasília]. University of Brasília (in Portuguese).

Cordeiro, A.F.B. (2007). *Avaliação numérica de reforço de grupo de estacas pela introdução de estacas adicionais* [Master's dissertation]. University of Brasília (in Portuguese).

Cunha, R.P., Cordeiro, A.F.B., & Sales, M.M. (2010). Numerical assessment of an imperfect pile group with a defective pile in both initial and reinforced conditions. *Soils and Rocks*, 33(2), 81-93. http://doi.org/10.28927/SR.332081.

Cunha, R.P., Cordeiro, A.F.B., Sales, M.M., & Small, J.C. (2007). Parametric analyses of pile groups with defective piles: observed numerical behavior and remediation. In *10th Australia New Zealand Conference on Geomechanics* (pp. 454-459). Brisbane.

Décourt, L. (1993). Predicted and measured behavior of non-displacement piles in residual soils. In *2nd International Geotechnical Seminar on Deep Foundations on Bored and Auger Piles* (pp. 369-376). Rotterdam: A.A. Balkema,

Décourt, L. (1995). On the load-settlement behavior of piles. *Soils and Rocks*, 18(2), 93-112.

Freitas Neto, O. (2013). *Avaliação Experimental e Numérica de Radiers Estaqueados com Estacas Defeituosas em Solo Tropical do Brasil* [Doctoral thesis, University of Brasília]. University of Brasília (in Portuguese).

Freitas Neto, O., Cunha, R.P., Albuquerque, P.J.R., Garcia, J.R., & Santos Júnior, O.F. (2020). Experimental and numerical analyses of a deep foundation containing a single defective pile. *Latin American Journal of Solids*

and Structures, 17(3), e270. http://doi.org/10.1590/1679-78255827.

García, F.J.A., Cunha, R.P., Albuquerque, P.J.R., Farias, M.M., & Bernardes, H.C. (2023). Experimental and numerical behavior of horizontally loaded piled rafts with a defective pile. *Geotechnical and Geological Engineering*, 41(1), 429-439. http://doi.org/10.1007/s10706-022-02288-2.

Klingmüller, O., & Kirsch, F. (2004). A quality and safety issue for cast-in-place: 25 years of experience with low-strain integrity testing in Germany, from scientific peculiarity to today's practice. In J. A. DiMaggio & M. H. Hussein (Eds.), *Current practices and future trends in deep foundations* (pp. 202-221). Reston: American Society of Civil Engineers. http://doi.org/10.1061/40743(142)12.

Kong, L., & Zhang, L. (2004). Lateral or torsional failure modes in vertically loaded defective pile groups. In J. P. Turner & P. W. Mayne (Eds.), *GeoSupport 2004: drilled shafts, micropiling, deep mixing, remedial methods, and specialty foundation systems* (pp. 625-636). Reston: American Society of Civil Engineers. http://doi.org/10.1061/40713(2004)43.

Lee, J., Park, D., Park, D., & Park, K. (2015). Estimation of load-sharing ratios for piled rafts in sands that includes interaction effects. *Computers and Geotechnics*, 63, 306-314. http://doi.org/10.1016/j.compgeo.2014.10.014.

Leung, Y.F., Klar, A., & Soga, K. (2010). Theoretical study on the pile length optimization of pile groups and piled rafts. *Journal of Geotechnical and Geoenvironmental Engineering*, 136(2), 319-330. http://doi.org/10.1061/(ASCE)GT.1943-5606.0000206.

Poulos, H.G. (1997). Behaviour of pile groups with defective piles. In *14th International Conference Soil Mechanics Foundation Engineering* (pp. 871-876). Hamburg.

Poulos, H.G. (1999). Pile defects: influence on foundation performance. In *4th International Conference on Deep Foundation Practice Incorporation* (pp. 57-69). Singapore.

Poulos, H.G. (2001). Piled raft foundations: design and applications. *Geotechnique*, 51(2), 95-113. http://doi.org/10.1680/geot.2001.51.2.95.

Poulos, H.G. (2005). Pile behavior – Consequences of geological and construction imperfections. *Journal of Geotechnical and Geoenvironmental Engineering*, 131(5), 538-563. http://doi.org/10.1061/(ASCE)1090-0241(2005)131:5(538).

Soares, W.C. (2011). *Radier estaqueado com estacas hollow auger em solo arenoso* [Doctoral thesis, Federal University of Pernambuco]. Federal University of Pernambuco (in Portuguese).

Soares, W.C., Coutinho, R.Q., & Cunha, R.P. (2015). Piled raft with hollow auger piles founded in a Brazilian granular deposit. *Canadian Geotechnical Journal*, 52(8), 1005-1022. http://doi.org/10.1139/cgj-2014-0087.

Teixeira, A.H. (1996). Projeto e Execução de Fundações. In *III Seminário de Engenharia de Fundações Especiais e Geotecnia* (pp. 1-18). São Paulo.

Teixeira, A.H., & Godoy, N.S. (1996). Análise, projeto e execução de fundações rasas. In W. Hachich, F. F. Falconi, J. L. Saes, R. G. Q. Frota & C. S. Carvalho, S. Niyama (Eds.), *Fundações: teoria e prática*. PINI.

van der Veen, C. (1953). The bearing capacity of a pile. In *International conference on soil mechanics and foundation engineering* (pp. 367-376). Zurich.

Xu, K. (2000). *General analysis of pile foundations and application to defective piles* [Doctoral Thesis, University of Sydney]. University of Sydney.

Xu, M., Ni, P., Ding, X., & Mei, G. (2019). Physical and numerical modelling of axially loaded bored piles with debris at the pile tip. *Computers and Geotechnics*, 114, 103146. http://doi.org/10.1016/j.compgeo.2019.103146.

Yan, Z., Sun, X.P., Yang, Z.X., & Fu, D.F. (2020). Lateral bearing performance of a defective pile-supported wharf with batter piles. *Journal of Waterway, Port, Coastal, and Ocean Engineering*, 146(5), 04020035. http://doi.org/10.1061/(ASCE)WW.1943-5460.0000597.

Zhang, L., & Wong, E. (2007). Centrifuge modeling of large-diameter bored pile groups with defects. *Journal of Geotechnical and Geoenvironmental Engineering*, 133(9), 1091-1101. http://doi.org/10.1061/(ASCE)1090-0241(2007)133:9(1091).